

See discussions, stats, and author profiles for this publication at: <https://www.researchgate.net/publication/231621951>

Trichloromethyl Chloroformate (“Diphosgene”), ClC(O)OCCl_3 : Structure and Conformational Properties in the Gaseous and Condensed Phases

ARTICLE in THE JOURNAL OF ORGANIC CHEMISTRY · APRIL 2006

Impact Factor: 4.72 · DOI: 10.1021/jo052260a

CITATIONS

5

READS

72

5 AUTHORS, INCLUDING:



Valeria B Arce

National University of La Plata

15 PUBLICATIONS 63 CITATIONS

SEE PROFILE



Carlos O. Della Vedova

National University of La Plata

293 PUBLICATIONS 2,678 CITATIONS

SEE PROFILE



Anthony J Downs

University of Oxford

258 PUBLICATIONS 5,070 CITATIONS

SEE PROFILE



Rosana Romano

National University of La Plata

116 PUBLICATIONS 863 CITATIONS

SEE PROFILE

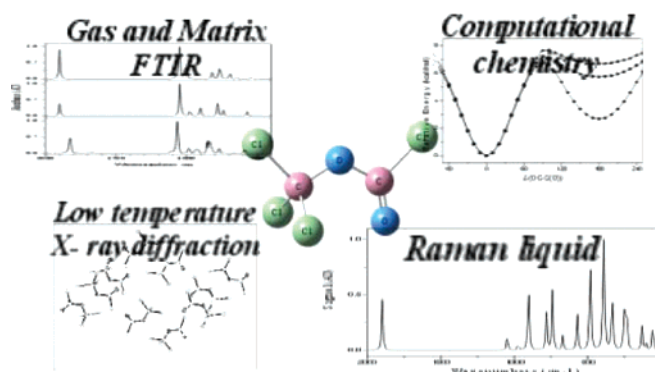
Trichloromethyl Chloroformate (“Diphosgene”), $\text{ClC}(\text{O})\text{OCCl}_3$: Structure and Conformational Properties in the Gaseous and Condensed Phases

Valeria B. Arce,[†] Carlos O. Della Védova,^{*,†,‡} Anthony J. Downs,[§] Simon Parsons,^{||} and Rosana M. Romano^{*,†}

CEQUINOR (CONICET) and Laboratorio de Servicios a la Industria y al Sistema Científico (UNLP-CIC-CONICET), Departamento de Química, Facultad de Ciencias Exactas, Universidad Nacional de La Plata, 47 esq. 115, (1900) La Plata, República Argentina, Inorganic Chemistry Laboratory, University of Oxford, South Parks Road, Oxford OX1 3QR, U.K., and Department of Chemistry, The University of Edinburgh, West Mains Road, Edinburgh EH9 3JJ, U.K.

romano@quimica.unlp.edu.ar; carlosdv@quimica.unlp.edu.ar

Received October 31, 2005



The conformational properties of gaseous trichloromethyl chloroformate (or “diphosgene”), $\text{ClC}(\text{O})\text{OCCl}_3$, have been studied by vibrational spectroscopy [IR (gas), IR (matrix), and Raman (liquid)] and quantum chemical calculations (MP2 and B3LYP with 6-311G* basis sets); in addition, the structure of a single crystal at low temperature has been determined by X-ray diffraction. $\text{ClC}(\text{O})\text{OCCl}_3$ exhibits only one conformational form having C_s symmetry with a synperiplanar orientation of the C–O single bond relative to the C=O double bond. The calculated energy difference between the *syn* and *anti* forms, 5.73 kcal mol^{−1} (B3LYP) or 7.06 kcal mol^{−1} (MP2), is consistent with the experimental findings for the gas and liquid phases. The crystalline solid at 150 K [monoclinic, $P2_1/n$, $a = 5.5578(5)$ Å, $b = 14.2895(12)$ Å, $c = 8.6246(7)$ Å, $\beta = 102.443(2)^\circ$, $Z = 4$] likewise consists only of molecules in the *syn* form.

1. Introduction

Trichloromethyl chloroformate or “diphosgene”, $\text{ClC}(\text{O})\text{OCCl}_3$, has been known since World War I because of its regrettable use, in common with that of phosgene, OCCl_2 , in chemical warfare. It acts as an easy-to-handle substitute for phosgene, to which its charcoal-catalyzed decomposition leads and which finds use in the preparation of a variety of chemical intermediates, e.g., isocyanates, carbonates, chloroformates, and *N*-carboxy anhydrides.¹ Aside from its well-documented toxicity,

phosgene can be formed in the atmosphere and indeed occurs in the stratosphere; its photolability causes it to have a lifetime of only about 13 years in the troposphere.²

Surprisingly little is known, however, about diphosgene itself. Thus, neither its structure nor its vibrational properties have been reported to date. Although the thermal decomposition of alkyl (*R*)-chloroformates $\text{ClC}(\text{O})\text{OR}$ gives RCl and CO_2 in what

[†] CEQUINOR (CONICET), Universidad Nacional de La Plata.

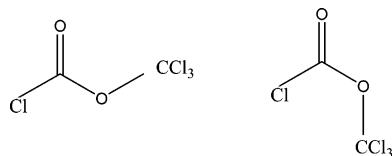
[‡] Laboratorio de Servicios a la Industria y al Sistema Científico (UNLP-CIC-CONICET), Universidad Nacional de La Plata.

[§] University of Oxford.

^{||} The University of Edinburgh.

(1) Kirk-Othmer Encyclopedia of Chemical Technology, 4th ed.; Wiley-Interscience: New York, 1996; Vol. 18, p 645. Kurita, K.; Iwakura, Y. *Org. Synth.* **1980**, 59, 195. Ueda, M.; Oikawa, H.; Kawaharasaki, N.; Imai, Y. *Bull. Chem. Soc. Jpn.* **1983**, 56, 2485. Katakai, R.; Iizuka, Y. *J. Org. Chem.* **1985**, 50, 715. Pridgen, L. N.; Prol, J., Jr.; Alexander, B.; Gillyard, L. *J. Org. Chem.* **1989**, 54, 3231.

(2) Helas, G.; Wilson, S. R. *Atmos. Environ., Part A* **1992**, 26, 2975.

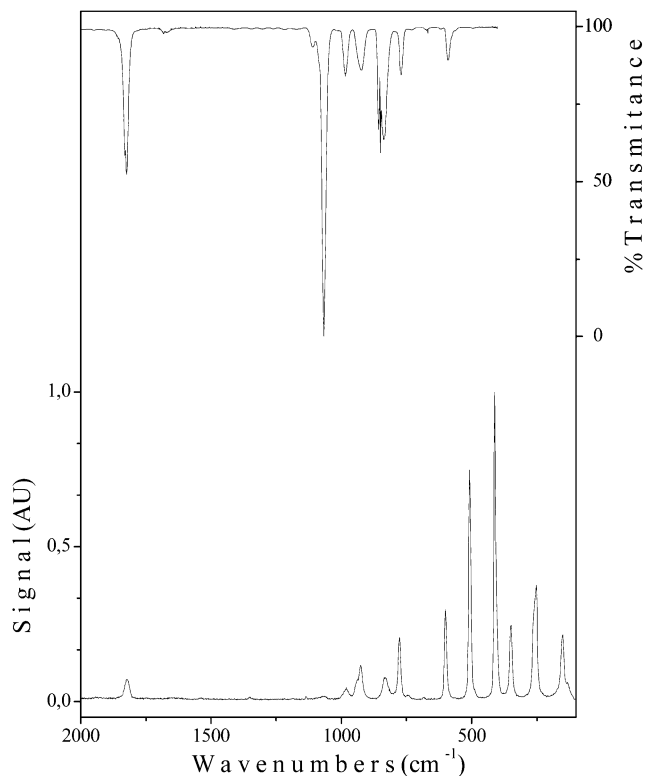
CHART 1. Representation of the *syn* (Left) and *anti* (Right) Conformers of ClC(O)OCCl_3 

is considered to be an $\text{S}_{\text{N}}1$ process,³ gaseous ClC(O)OCCl_3 decomposes at 300 °C not to the expected products CCl_4 and CO_2 , but to phosgene. This behavior has been explained by the low stability of the $\text{S}_{\text{N}}1$ transition state for $\text{R} = \text{CCl}_3$.⁴ The inductive effect of the CCl_3 group in diphosgene, reinforced by that of the Cl atom attached to the carbonyl carbon atom, promotes dissociation to phosgene.⁵ Otherwise, Wallington et al.⁶ have reported on experiments involving mixtures of ClC(O)OCH_3 and Cl_2 diluted with N_2 and designed to study the chain chlorination of ClC(O)OCH_3 . Following successive periods of UV irradiation, the IR bands due to ClC(O)OCH_3 decreased, and according to the simplest interpretation, new bands attributable to the three products $\text{ClC(O)OCH}_2\text{Cl}$, ClC(O)OCHCl_2 , and ClC(O)OCCl_3 were observed to develop. Pasquato et al.⁷ have also reported that diphosgene is an intermediate in the decomposition of “triphosgene”, $\text{O}=\text{C}(\text{OCCl}_3)_2$, to phosgene brought about by the action of chloride ions; in this case, too, the reaction was conveniently monitored by IR measurements.

Here, we present the results of an experimental investigation of the structure and vibrational properties of diphosgene, ClC(O)OCCl_3 . Thus, the IR spectra of the vapor alone at room temperature and isolated in a solid Ar matrix at ca. 15 K and the Raman spectrum of the liquid have been measured and analyzed. In principle, the diphosgene molecule can possess two conformations, one with *syn* and the other with *anti* orientation of the C–O single bond with respect to the C=O double bond (Chart 1). Ab initio (MP2) and DFT (B3LYP) quantum chemical calculations indicate that the *syn* conformer is significantly more stable than the *anti* conformer, a conclusion consistent with the vibrational spectra of the gas and liquid, and indeed, this is the only form present in a single crystal at 150 K, as determined by X-ray analysis.

2. Results

(i) Quantum Chemical Calculations. The two possible conformations of the ClC(O)OCCl_3 molecule depend on the torsional position of the OCCl_3 group with respect to the O–C(O) single bond; the orientations can be *syn* or *anti* [$\varphi(\text{O}=\text{C}-\text{O}-\text{C}) = 0$ or 180° , respectively]. Geometry optimizations were performed with the program suite Gaussian 98 software package⁸ for various fixed torsional angles $\varphi(\text{O}=\text{C}-\text{O}-\text{C})$ around the O–C(O) bond using either the MP2 approximation or DFT/B3LYP method, in each case with 6-311G* basis sets. The resulting potential function for internal rotation possesses two minima, one corresponding to the *syn* [$\varphi(\text{O}=\text{C}-\text{O}-\text{C}) = 0^\circ$]

**FIGURE 1.** Vibrational spectra of ClC(O)OCCl_3 . Upper trace: IR spectrum of the vapor at ca. 1 Torr and room temperature. Lower trace: Raman spectrum of the liquid at room temperature.

and the other to the *anti* [$\varphi(\text{O}=\text{C}-\text{O}-\text{C}) = 180^\circ$] form, with the former being more stable than the latter by $\Delta E^\circ = 5.73 \text{ kcal mol}^{-1}$ (B3LYP) or $7.06 \text{ kcal mol}^{-1}$ (MP2). In either case, the calculations anticipate that only the *syn* conformer will be present in appreciable concentrations in the gas phase at ambient temperatures.

(ii) Vibrational Spectra. The IR spectrum of gaseous ClC(O)OCCl_3 and the Raman spectrum of the liquid are shown in Figure 1. Details of the spectra are itemized in Table 1, together with those of the IR spectrum of an Ar matrix at ca. 15 K doped with the vapor ($\text{ClC(O)OCCl}_3/\text{Ar} = 1:1000$), and the wavenumbers, IR and Raman intensities calculated for *syn*- and *anti*- ClC(O)OCCl_3 at the DFT/B3LYP/6-311G* level of the theory. All the vibrational modes of diphosgene are active in both IR absorption and Raman scattering, being classified as $12 \text{ A}' + 6 \text{ A}''$ in the C_s symmetry point group appropriate to the ClC(O)OCCl_3 molecule.

Figure 2 compares the measured IR spectrum of the vapor (lower trace) with both *syn* (middle trace) and *anti* (upper trace) spectra calculated according to the B3LYP method. Figure 3 repeats this comparison for the Raman spectra. There is good

(3) Hughes, E. D.; Ingold, C. K.; Whitfield, I. C. *Nature* **1941**, 147, 206.
(4) Ramsberger, H. C.; Waddington, G. *J. Am. Chem. Soc.* **1948**, 55, 214.

(5) Hales, J. L.; Idris Jones, J.; Kynaston, W. *J. Chem. Soc.* **1957**, 618.
(6) Wallington, T. J.; Hurley, M. D.; Maurer, T.; Barnes, I.; Becker, K. H.; Tyndall, G. S.; Orlando, J. J.; Pimentel, A.-S.; Bilde, M. *J. Phys. Chem. A* **2001**, 105, 5146.

(7) Pasquato, L.; Modena, G.; Cotarca, L.; Delogu, P.; Mantovani, S. *J. Org. Chem.* **2000**, 65, 8224.

(8) Frisch, M. J.; Trucks, G. W.; Schlegel, H. B.; Scuseria, G. E.; Robb, M. A.; Cheeseman, J. R.; Zakrzewski, V. G.; Montgomery, J. A., Jr.; Stratmann, R. E.; Burant, J. C.; Dapprich, S.; Millam, J. M.; Daniels, A. D.; Kudin, K. N.; Strain, M. C.; Farkas, O.; Tomasi, J.; Barone, V.; Cossi, M.; Cammi, R.; Mennucci, B.; Pomelli, C.; Adamo, C.; Clifford, S.; Ochterski, J.; Petersson, G. A.; Ayala, P. Y.; Cui, Q.; Morokuma, K.; Malick, D. K.; Rabuck, A. D.; Raghavachari, K.; Foresman, J. B.; Cioslowski, J.; Ortiz, J. V.; Baboul, A. G.; Stefanov, B. B.; Liu, G.; Liashenko, A.; Piskorz, P.; Komaromi, I.; Gomperts, R.; Martin, R. L.; Fox, D. J.; Keith, T.; Al-Laham, M. A.; Peng, C. Y.; Nanayakkara, A.; Gonzales, C.; Challacombe, M.; Gill, P. M. W.; Johnson, B.; Chen, W.; Wong, M. W.; Andres, J. L.; Head-Gordon, M.; Replogle, E. S.; Pople, J. A. *Gaussian 98*, Revision A.7; Gaussian, Inc.: Pittsburgh, PA, 1998.

TABLE 1. Observed and Calculated Vibrational Data for ClC(O)OCCl₃ (cm⁻¹)

experimental			calculated ^d						mode symmetry/assign/aprox description of mode
IR ^a	Raman ^b	Ar matrix ^c	syn			anti			
			ν	IR ^e	Ra	ν	IR ^e	Ra	
1823 (33)	1822 (12)	1821 1819 1815 (80)	1898	36 (324)	55	1900	61 (467)	100	A' ν (C=O)
1109 (4)									
1067 (100)		1070 1068 1066 1064 1061 (100)	1048	100 (896)	18	1054	100 (768)	35	A' ν_{as} (C–O–C)
985 (8)	982 (6)	997 990 987 985 983 981 (34) 978 974 973	976	18 (160)	<1	1005	42 (323)	<1	A' ν_{s} (C–O–C)
923 (22)	938 (11) 926 (15)	936 933 930 929 925 921 (28) 920 918	903	29 (258)	82	818	18 (139)	25	A' ν_{as} (CCl ₃)
832 (39)	833 (13)	837 837 824 823(77) 822	781	33 (300)	36	766	37 (282)	25	A'' ν_{as} (CCl ₃)
770 (12)	778 (23)	772 770 768(29)	739	16 (141)	55	693	16 (124)	25	A' ν (C–Cl)
668 (<1)		672 (9)	669	<1 (1)	18	643	3 (26)	<1	A'' ρ (Cl–C=O)
590 (10)	600 (30)	594 592 591 (25) 589	571	12 (110)	36	536	5 (40)	35	A' ν_{s} (CCl ₃)
	508 (74)		483	<1 (5)	100	497	2 (13)	45	A' δ (O=C–Cl)
	411 (100)		393	<1 (<1)	100	422	<1 (5)	50	A' δ_{s} (CCl ₃)
			386	<1 (2)	36	379	<1 (2)	25	A'' δ_{as} (CCl ₃)
	350 (27)		333	<1 (2)	64	301	<1 (<1)	35	A' ρ (CCl ₃)
			252	<1 (<1)	36	294	<1 (<1)	30	A'' ρ (CCl ₃)
	253 (66)		243	<1 (<1)	18	252	<1 (<1)	15	A' δ (O–C–Cl ₃)
			233	<1 (<1)	36	217	<1 (<1)	15	A' δ (Cl–CO)
	152 (23)		130	<1 (<1)	27	137	<1 (<1)	<1	A' δ (C–O–C)
			102	<1 (<1)	<1	99	<1 (<1)	<1	A'' τ (O–C=OCl)
			56	<1 (<1)	27	32	<1 (<1)	15	A'' τ (C–Cl ₃)

^a Gas phase. The relative absorbance at band maximum is shown in parentheses. ^b Liquid, room temperature. ^c ClC(O)OCCl₃/Ar (1/1000). ^d B3LYP (6-311G*). ^e Values in parentheses are in km/mol.

agreement, as regards both wavenumbers and relative intensities, between the observed and calculated vibrational spectra for the *syn* form. The bands in the observed spectra have then been assigned on the basis of comparisons (i) with the calculated IR spectrum and (ii) with the spectra of related molecules, most notably ClC(O)OCF₃⁹ and FC(O)OCF₃,¹⁰ but also taking account of species such as ClC(O)OSO₂CF₃¹¹ and CCl₃SCN.¹² The approximate descriptions of the modes given in Table 1

are based on the displacement vectors for the relevant fundamentals derived from the B3LYP calculations.

The most intense IR absorption of the vapor occurs at 1067 cm⁻¹ and that of the matrix at 1061 cm⁻¹, respectively, in agreement with the calculated value of 1048 cm⁻¹. This can be identified with what is essentially the C–O–C antisymmetric stretching fundamental. The measured IR spectra include two other strong bands near 923 and 830 cm⁻¹, which are assigned to antisymmetric CCl₃ stretching modes.

(9) Erben, M. F.; Della Vedova, C. O.; Boese, R.; Willner, H.; Oberhammer, H. *J. Phys. Chem. A* **2004**, *108*, 699.

(10) Hermann, A.; Trautner, F.; Gholivand, K.; von Ahsen, S.; Varetto, E. L.; Della Vedova, C. O.; Willner, H.; Oberhammer, H. *Inorg. Chem.* **2001**, *40*, 3979.

(11) Della Vedova, C. O.; Downs, A. J.; Moschione, E.; Parsons, S.; Romano, R. M. *Inorg. Chem.* **2004**, *43*, 8143.

(12) Ullrich, S. E.; Di Napoli, F.; Hermann, A.; Della Vedova, C. O. *J. Raman Spectrosc.*, **2000**, *31*, 909.

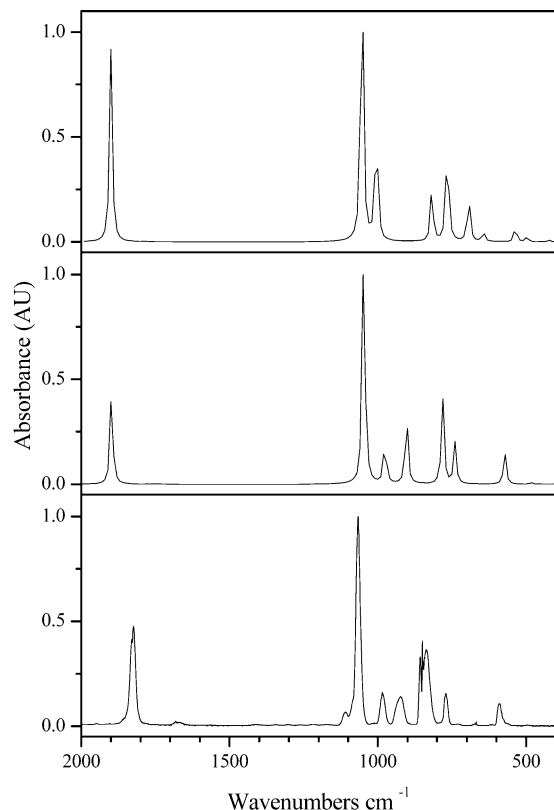


FIGURE 2. FTIR spectra of ClC(O)OCCl_3 . Lower trace: IR spectrum of the vapor at ca. 1 Torr and ambient temperature. Medium trace: simulated infrared spectrum for the *syn* conformer from B3LYP/6-311G*. Upper trace: simulated infrared spectrum for the *anti* conformer from B3LYP/6-311G*

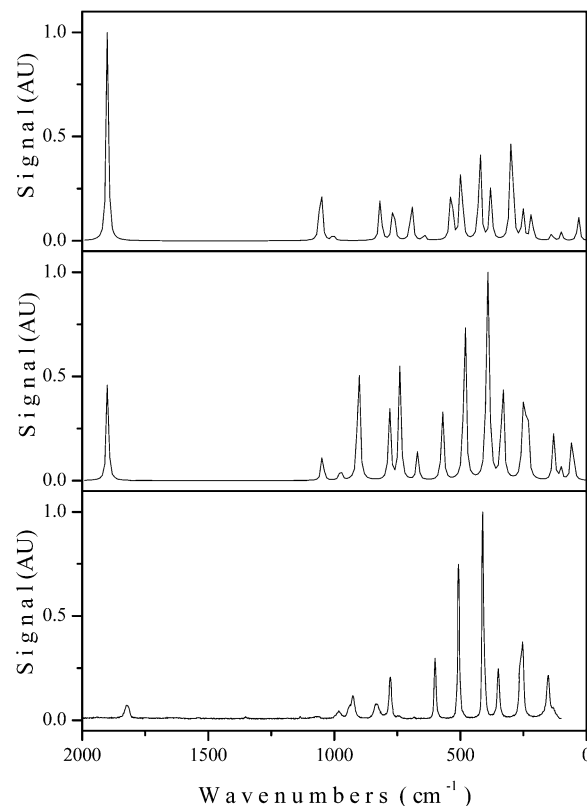


FIGURE 3. Raman spectra of ClC(O)OCCl_3 . Lower trace: Raman spectrum of the liquid at room temperature. Medium trace: simulated infrared spectrum for the *syn* conformer from B3LYP/6-311G*. Upper trace: simulated infrared spectrum for the *anti* conformer from B3LYP/6-311G*

The $\text{C}=\text{O}$ stretching regions of the IR spectra recorded (a) for the matrix-isolated molecules and (b) for the vapor at ambient temperatures are illustrated in Figure 4. The band associated with the $\nu(\text{C}=\text{O})$ mode centered at 1823 cm^{-1} in the vapor spectrum can be described as having a B-type contour. This is wholly consistent with the properties of *syn*- ClC(O)OCCl_3 in which the $\nu(\text{C}=\text{O})$ oscillator is almost parallel to the *B* axis, as illustrated in Figure 5. By contrast, the *anti* conformer would be expected to give a $\nu(\text{C}=\text{O})$ absorption either with an A- or AB-hybrid contour. Although the corresponding band in the matrix spectrum showed splitting, this is almost certainly due to matrix site effects, and neither the vapor nor the matrix spectrum gave any hint of a second $\nu(\text{C}=\text{O})$ band that might signal the presence of the *anti* conformer.

The change from the gas or matrix to the liquid phase produces little or no change in the $\nu(\text{C}=\text{O})$ wavenumber, as evidenced by the Raman spectrum which witnesses a single band of medium intensity at 1822 cm^{-1} . The most intense Raman scattering of the liquid was observed to occur at 600, 508, 411, 350, and 253 cm^{-1} . Comparison with the results of the B3LYP calculations suggests that these correspond to $\nu_s(\text{CCl}_3)$, $\delta(\text{O}=\text{C}-\text{Cl})$, $\delta_s(\text{CCl}_3)$, $\rho(\text{CCl}_3)$, and $\delta(\text{OCCl}_3)$ modes, respectively.

No appreciable change in the IR spectrum was observed when the Ar matrix was irradiated with broad-band UV–visible light ($200 \leq \lambda \leq 800\text{ nm}$) for up to 60 min. The intensities of the IR absorptions due to the ClC(O)OCCl_3 molecules remained almost constant, and no new absorptions were observed to develop. The UV–vis spectrum of the vapor showed absorptions in the range 200–300 nm, and it seems unlikely that the molecule is

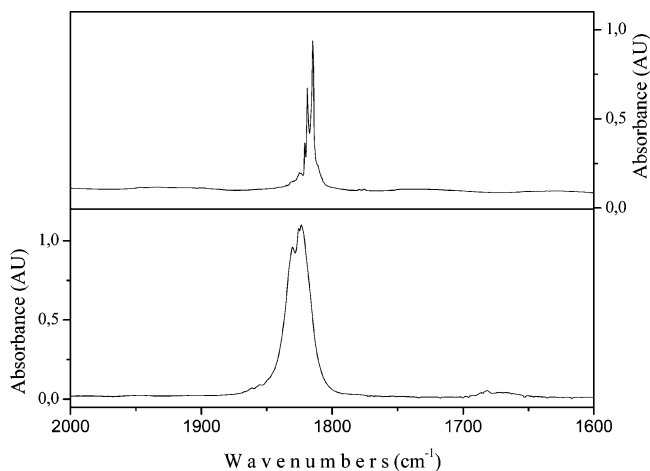


FIGURE 4. $\text{C}=\text{O}$ stretching region of the IR spectrum of ClC(O)OCCl_3 . Lower trace: IR spectrum of the vapor. Upper trace: IR spectrum of a solid Ar matrix [$\text{ClC(O)OCCl}_3/\text{Ar} = 1:1000$] at ca. 15 K.

photostable with respect to UV light. The failure to witness any change in the matrix probably reflects the relatively large size of the parent molecule and its decomposition products, causing photodissociation to be inhibited by the matrix cages.

(iii) Crystal Structure. Essential details of the X-ray analysis carried out on a single crystal of the title compound at 150 K are available in the Supporting Information. A sample of trichloromethyl chloroformate was held in a Pyrex capillary and a single crystal grown in situ by Boese's laser-assisted zone-

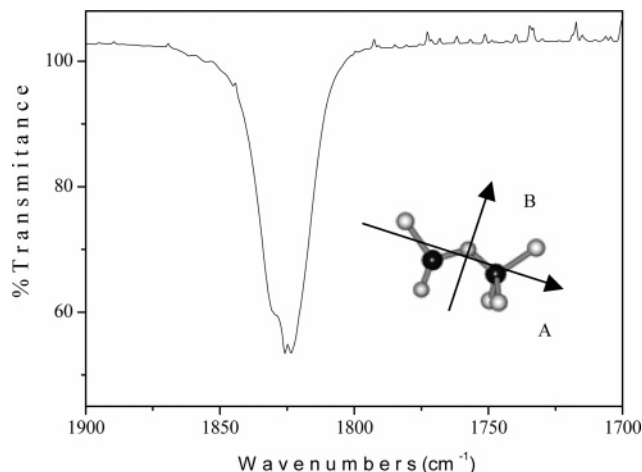


FIGURE 5. Principal axes of inertia (A and B) for the *syn* conformer of ClC(O)OCCl_3 (the C axis is perpendicular to the molecular symmetry plane) and IR absorption of ClC(O)OCCl_3 vapor associated with the $\nu(\text{C}=\text{O})$ fundamental.

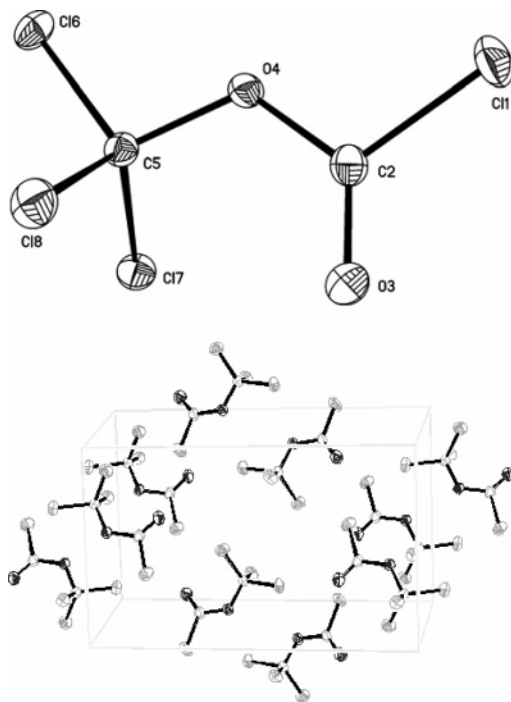


FIGURE 6. Upper trace: Molecular structure of the *syn* conformer of ClC(O)OCCl_3 as observed in the crystal structure. Ellipsoids enclose 30% probability surfaces. Lower trace: Packing of molecules in crystalline ClC(O)OCCl_3 .

refinement method.¹³ Hence, the compound was found to crystallize in the monoclinic space group $P2_1/n$, with unit cell dimensions $a = 5.5578(5)$ Å, $b = 14.2895(12)$ Å, $c = 8.6246(7)$ Å, and $\beta = 102.443(2)^\circ$. The packing is made up of four ClC(O)OCCl_3 molecules per unit cell, each adopting the *syn* conformation illustrated (see Figure 6). The molecule adopts the *syn* conformation; i.e., *syn* is the more stable form of the isolated molecule on the evidence of the calculations and the

TABLE 2. Experimental and Calculated Geometric Parameters for ClC(O)OCCl_3^a

parameter	X-ray	B3LYP ^b	MP2 ^b
C11–C2	1.729(1)	1.762	1.739
C2–O3	1.1802(12)	1.177	1.186
C2–O4	1.365(1)	1.366	1.366
O4–C5	1.419(1)	1.404	1.409
C5–Cl6	1.7629(8)	1.785	1.762
C5–Cl7	1.7633(9)	1.793	1.769
C5–Cl8	1.7620(9)	1.793	1.769
C11–C2–O3	124.80(7)	124.96	125.24
C11–C2–O4	107.34(6)	106.88	106.75
O3–C2–O4	127.86(9)	128.16	128.01
C2–O4–C5	118.23(7)	120.73	118.73
O4–C5–Cl6	103.98(6)	103.97	103.41
O4–C5–Cl7	111.28(6)	111.40	111.08
Cl6–C5–Cl7	109.84(4)	109.80	110.13
O4–C5–Cl8	110.92(6)	111.40	111.07
Cl6–C5–Cl8	109.44(5)	109.79	110.13
Cl7–C5–Cl8	111.15(5)	110.30	110.79

^a Bond lengths in Å, bond angles in deg. ^b Using 6-311G* basis sets.

preferred form in the vapor phase. The *anti* form presents a larger dipole moment than the *syn* form according to our theoretical calculations (1.56 and 0.85 D, respectively, using the B3LYP/6-311G*). It is known that a rotamer with a larger dipole moment is always likely to be stabilized in the solid state. Consequently, packing effects would appear to stabilize the *syn* form in the solid. Thus, whereas the more stable conformer for the isolated molecules would tend to stabilize the *syn* form, polarization effects would tend to favor the *anti* form, and packing effects would stabilize the *syn* rotamer in the solid state. The packing involves no significant intermolecular interactions, all the contacts being at distances in excess of the sums of the relevant van der Waals radii. In these circumstances, it is perhaps not surprising that the molecular dimensions determined by experiment and listed in Table 2 match well those calculated using MP2 or B3LYP methods.

3. Discussion

As indicated in the Introduction, this report provides the first characterization of the structure and vibrational properties of the trichloromethyl chloroformate (diphosgene) molecule, ClC(O)OCCl_3 . Our quantum chemical calculations indicate that gaseous ClC(O)OCCl_3 should exist at room temperature essentially as a single conformer with a synperiplanar orientation of the C–O single bond relative to the C=O double bond, this being more stable than the alternative *anti* conformer by 6–7 kcal mol^{−1}. The IR spectrum of the vapor is consistent with this expectation, and the Raman spectrum implies that the *syn* conformer is also the sole component of the liquid. Comparisons given in the Figures 2 and 3 between experimental and calculated vibrational spectra act as further confirmation that only the *syn* form exists. The structure of a single crystal at 150 K confirms that the same conformer is favored in the solid state, with dimensions that are well reproduced by the quantum chemical calculations.

Figure 7 shows the potential energy curves calculated (B3LYP/6-311G*) for internal rotation around the C–O bond of XC(O)OCCl_3 for X = F, Cl, and Br [FC(O)OCCl_3 having recently been synthesized.¹⁴]. According to these results, the energy difference between the *syn* and *anti* forms is 2.66 kcal

(13) Boese, R.; Nussbaumer, M. In *Correlations, Transformations, and Interactions in Organic Crystal Chemistry*; Jones, D. W., Katrusiak, A., Eds.; IUCr Crystallographic Symposia, Vol. 7; Oxford University Press: Oxford, U.K., 1994; p 20.

(14) Romano, R. M.; Arce, V. B. To be published.

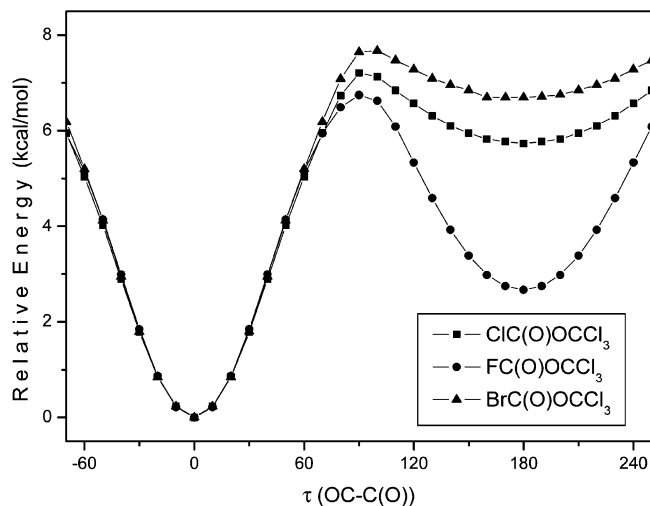


FIGURE 7. Potential energy curve for an XC(O)OCCl_3 molecule ($\text{X} = \text{F}, \text{Cl}$ or Br) as a function of the $\tau[\text{OC}-\text{C(O)}]$ dihedral angle calculated with the B3LYP/6-311G* approximation.

mol^{-1} for FC(O)OCCl_3 , $5.73 \text{ kcal mol}^{-1}$ for ClC(O)OCCl_3 , and $6.70 \text{ kcal mol}^{-1}$ for BrC(O)OCCl_3 . Donor/acceptor electronic interactions apart, it appears that other factors, notably steric repulsion between the CCl_3 group and the X atom, must play an important role in determining the energy balance between the two forms. Such steric repulsion destabilizes the *anti* conformer to an extent that increases as the X atom becomes bigger.⁹ The trend can also be rationalized on the basis of the anomeric effect. Some topics treated in this work are closely related with those reported elsewhere.¹⁵

4. Experimental Section

Purification and Physical Properties. The trichloromethyl chloroformate was a commercial product. It was purified by fractionating the volatile components under dynamic vacuum through traps held at -30 , -60 , -90 , and -196 °C. The pure compound remains in the -30 °C trap. Its purity was checked using NMR and vibrational spectroscopy.

Spectroscopic Characterization. Details of the vibrational spectra of the compound have already been presented (see Table 1 and Figures 1–5). Raman spectra were excited at $\lambda = 632.8 \text{ nm}$ with a He–Ne laser and measured with a spectrometer having a CCD detector, typically at a resolution of 2 cm^{-1} . Gas mixtures of ClC(O)OCCl_3 with argon (BOC, research grade) in proportions ca. 1:1000, prepared by standard manometric methods, were deposited on a CsI window cooled to ca. 15 K by means of a closed-cycle refrigerator using the pulsed deposition technique.^{16,17} IR spectra of the matrix samples were recorded in the range $4000\text{--}400 \text{ cm}^{-1}$ at a resolution of 0.5 cm^{-1} , with 256 scans and a wavenumber accuracy of $\pm 0.1 \text{ cm}^{-1}$. FTIR instrument equipped with an MCTB detector. Following deposition and IR analysis of the resulting matrix, the IR spectrum was also used to explore the effect of exposing the sample to broad-band UV–vis radiation ($200 \leq \lambda \leq 800 \text{ nm}$) supplied by a Hg–Xe arc lamp operating at 800 W. The same IR spectrometer was used to record the IR spectrum of ClC-

$(\text{O})\text{OCCl}_3$ vapor contained at a pressure of ca. 1 Torr in a Pyrex-bodied cell fitted with CsI windows and having a path length of ca. 100 mm.

In addition, the UV–vis spectrum of the vapor of the compound (contained in a Pyrex cell fitted with quartz windows and with a path length of 100 mm) was recorded with a Perkin-Elmer Lambda 900 spectrophotometer. Absorptions were observed with maxima centered at 210, 257, and 298 nm and extinction coefficients of 323, 596, and $79 \text{ L mol}^{-1} \text{ cm}^{-1}$, respectively.

Crystal Structure. A single crystal of ClC(O)OCCl_3 was grown at 200 K within a Pyrex capillary using an OHCD laser-assisted crystallizer,¹³ the capillary being mounted on a special diffractometer equipped with a low-temperature device.¹⁸ Diffraction measurements were then made on the crystal cooled to 150 K; essential details are shown in the Supporting Information. Following integration, data reduction, and application of an absorption correction,¹⁹ the structure was solved by direct methods²⁰ and refined by full-matrix least-squares against F using 1482 data with $F > 4\sigma(F)$.²¹ Other calculations were accomplished using another program.²² All atoms were modeled with anisotropic displacement parameters. Of 4195 data collected, 1594 were unique ($R_{\text{int}} = 0.027$). The final R and R_w were 0.0248 and 0.0271, respectively. The final difference map extrema were $+0.48$ and $-0.39 \text{ e } \text{\AA}^{-3}$.

Theoretical Calculations. All the quantum chemical calculations were performed using the Gaussian 98 program package⁸ under the Linda parallel execution environment using two coupled PC's. Geometry optimizations were sought (i) with B3LYP methods, and (ii) with MP2 methods; in all cases, the calculations employed 6-311G* basis sets and standard gradient techniques with simultaneous relaxation of all the geometric parameters.

Acknowledgment. Financial support by the Volkswagen Stiftung is gratefully acknowledged. C.O.D.V. and R.M.R. acknowledge the Fundación Antorchas, Alexander von Humboldt, DAAD (Deutscher Akademischer Austauschdienst, Germany), Agencia Nacional de Promoción Científica y Técnica (ANPCYT), Consejo Nacional de Investigaciones Científicas y Técnicas (CONICET), Comisión de Investigaciones de la Provincia de Buenos Aires (CIC), Facultad de Ciencias Exactas (UNLP), and Jesus College Oxford for financial support. R.M.R. is also indebted to the Royal Society of Chemistry for a grant for international authors. A.J.D. and S.P. are grateful to the EPSRC of the UK for funding the purchase of equipment. C.O.D.V. especially acknowledges the DAAD for its generous sponsorship of the DAAD Regional Program of Chemistry of the Republic of Argentina (supporting Latin-American students for a Ph.D. program in La Plata).

Supporting Information Available: X-ray crystallographic data (CIF), atomic coordinates and equivalent isotropic displacement parameters, anisotropic displacement parameters, crystal data, structure refinement details, and ^{13}C NMR spectrum of ClC(O)OCCl_3 . GAUSSIAN output with the atomic coordinates, number of imaginary frequencies and total energy for *syn*- and *anti*- ClC(O)OCCl_3 calculated with B3LYP/6-311G*. This material is available free of charge via the Internet at <http://pubs.acs.org>.

JO052260A

(18) Cosier, J.; Glazer, A. M. *J. Appl. Crystallogr.* **1986**, *19*, 105.

(19) Sheldrick, G. M. *SADABS*; University of Göttingen: Göttingen, Germany, 2002.

(20) Beurskens, P. T.; Beurskens, G.; Bosman, W. P.; de Gelder, R.; García-Granda, S.; Gould, R. O.; Israël, R.; Smits, J. M. M. *Crystallography Laboratory*, University of Nijmegen, Toernooiveld 1, 6525 ED Nijmegen, The Netherlands, 1996.

(21) Betteridge, P. W.; Carruthers, J. R.; Cooper, R. I.; Prout, K.; Watkin, D. J. *J. Appl. Crystallogr.* **2003**, *36*, 1487.

(22) Spek, A. L. *PLATON – A Multipurpose Crystallographic Tool*; Utrecht University: Utrecht, The Netherlands, 2003. PC version in WINGX: Farrugia, L. J. *J. Appl. Crystallogr.* **1999**, *32*, 837.

(15) Pawar, D. M.; Sims, Y. S.; Moton D. M.; Noe, E. A. *THEOCHEM* **2003**, *626*, 159.

(16) See for example: Romano, R. M.; Della Védova, C. O.; Downs, A. J.; Greene, T. M. *J. Am. Chem. Soc.* **2001**, *123*, 5794 and references therein.

(17) Perutz, R. N.; Turner, J. J. *J. Chem. Soc., Faraday Trans. 2* **1973**, *69*, 452.